High spatiotemporal resolution assessment for the impact of historical wetland loss on current wetland change trajectory using time series optical remote sensing and SAR data – a case study in Zhenlai County, Jilin Province, China.

Table S1. The parameters derived from the Sentinel sensor [1–3].

Parameters	**Data Resource and Platform**	**Method of Calculation**
NDVI	Sentinel-2, GEE	$\mathrm{NDVI} = \frac{\mathrm{B_{NIR}} - \mathrm{B_{red}}}{\mathrm{B_{NIR}} + \mathrm{B_{red}}}$
EVI		$\mathrm{EVI} = \frac{2.5 \times (\mathrm{B_{NIR}} - \mathrm{B_{red}})}{\mathrm{B_{NIR}} + 6 \times \mathrm{B_{red}} - 7.5 \times \mathrm{B_{blue}} + 1}$
LSWI		$\mathrm{LSWI} = \frac{\mathrm{B_{NIR}} - \mathrm{B_{SWIR}}}{\mathrm{B_{NIR}} + \mathrm{B_{SWIR}}}$
NDWI		$\mathrm{NDWI} = \frac{\mathrm{B_{green}} - \mathrm{B_{NIR}}}{\mathrm{B_{green}} + \mathrm{B_{NIR}}}$
mNDWI		$\mathrm{mNDWI} = \frac{\mathrm{B_{green}} - \mathrm{B_{SWIR}}}{\mathrm{B_{green}} + \mathrm{B_{SWIR}}}$
I_1, I_2	Sentinel-1, PolSARpro	The eigenvalues λ_1 and λ_2 of the coherency matrix $C_2 = \begin{bmatrix} C_{11} & C_{12} \\ C_{21} & C_{22} \end{bmatrix} = \begin{bmatrix} \langle \lvert S_{VV} \rvert^2 \rangle & \langle S_{VV} S_{VH}^* \rangle \\ \langle S_{VH} S_{VV}^* \rangle & \langle \lvert S_{VH} \rvert^2 \rangle \end{bmatrix}$ $\langle \cdot \rangle$: the spatial average over a selected window size *: the complex conjugate $S_{VV}\ and\ S_{VH}: the\ dual\ polarization\ complex\ SAR\ images$
Anisotropy		$A = \frac{\lambda_1 - \lambda_2}{\lambda_1 + \lambda_2}$
Entropy		$H = -P_1 log_2 P_1 - P_2 log_2 P_2$; $P_1 = \frac{\lambda_1}{\lambda_1 + \lambda_2}$; $P_2 = \frac{\lambda_2}{\lambda_1 + \lambda_2}$ $H: Entropy$ $P_i: the\ pseudo\ probabilities$

Alpha		$\bar{\propto}= P_1 \propto +P_2(\frac{\pi}{2}-\propto);\ \propto= \cos^{-1}\frac{\lvert\chi_1\rvert}{\lvert\upsilon_1\rvert}$ $\bar{\propto}$: Alpha, $the\ mean\ scattering\ angle$ $\propto$: $the\ scattering\ angle$
the derivatives of H and/or A		$SE = SE_I + SE_P;\ SE_I = 2\log(\frac{\pi eTr[C_2]}{2});\ SE_p = 4\log(\frac{det[C_2]}{Tr[C_2]^2})$ SE: Shannon entropy, SE_I: Shannon entropy in intensity, SE_P: Shannon entropy in polarizability HA, (1-H)(1-A), H(1-A), (1-H)A
σ^0	Sentinel-1, SARscape	$\sigma_{dB}^0 = 10 \times log_{10}(k_s \times \lvert DN\rvert^2) + 10 \times log_{10}(\sin\theta_{loc})$ σ_{dB}^0: $sigma\ naught\ values\ in\ dB$ k_s: $calibration\ and\ processor\ scalling\ factor$ DN: $digital\ number$ θ_{loc}: local incidence angle
CC		$\gamma = \frac{\langle S_1 S_2^*\rangle}{\sqrt{\langle S_1 S_1^*\rangle\langle S_{21} S_2^*\rangle}}$ $S_1 and\ S_2$: $the\ complex\ pixel\ values\ of\ backscattering\ coefficier$

Table S2. Number of the ROI and classification accuracies during 1985 to 2018.

Year	the Number of the Maps (Landsat 5, 7, 8)	the Number of ROI	Overall Accuracy	Kappa
1985	26, 0, 0	516	0.86	0.83
1986	38, 0, 0	558	0.86	0.83
1987	46, 0, 0	512	0.84	0.80
1988	50, 0, 0	501	0.85	0.82
1989	50, 0, 0	508	0.89	0.87
1990	45, 0, 0	505	0.84	0.81
1991	53, 0, 0	502	0.87	0.85
1992	56, 0, 0	502	0.89	0.87
1993	41, 0, 0	500	0.89	0.87
1994	48, 0, 0	508	0.90	0.89
1995	44, 0, 0	520	0.89	0.87
1996	45, 0, 0	519	0.84	0.81
1997	53, 0, 0	523	0.88	0.86
1998	42, 0, 0	510	0.90	0.88
1999	11, 54, 0	506	0.92	0.90
2000	57, 60, 0	517	0.92	0.91
2001	60, 53, 0	553	0.87	0.85
2002	63, 44, 0	580	0.85	0.82
2003	44, 41, 0	578	0.88	0.86
2004	57, 55, 0	505	0.86	0.84
2005	49, 40, 0	501	0.86	0.83
2006	48, 53, 0	500	0.90	0.88
2007	54, 42, 0	511	0.87	0.84
2008	59, 34, 0	500	0.89	0.87
2009	44, 50, 0	501	0.92	0.90
2010	42, 42, 0	501	0.86	0.84
2011	47, 34, 0	502	0.92	0.91
2012	0, 52, 0	503	0.94	0.93
2013	0, 43, 43	502	0.92	0.91
2014	0, 64, 55	501	0.90	0.89
2015	0, 58, 46	502	0.95	0.94
2016	0, 51, 48	507	0.97	0.97
2017	0, 63, 46	521	0.92	0.91
2018	0, 67, 52	520	0.88	0.86

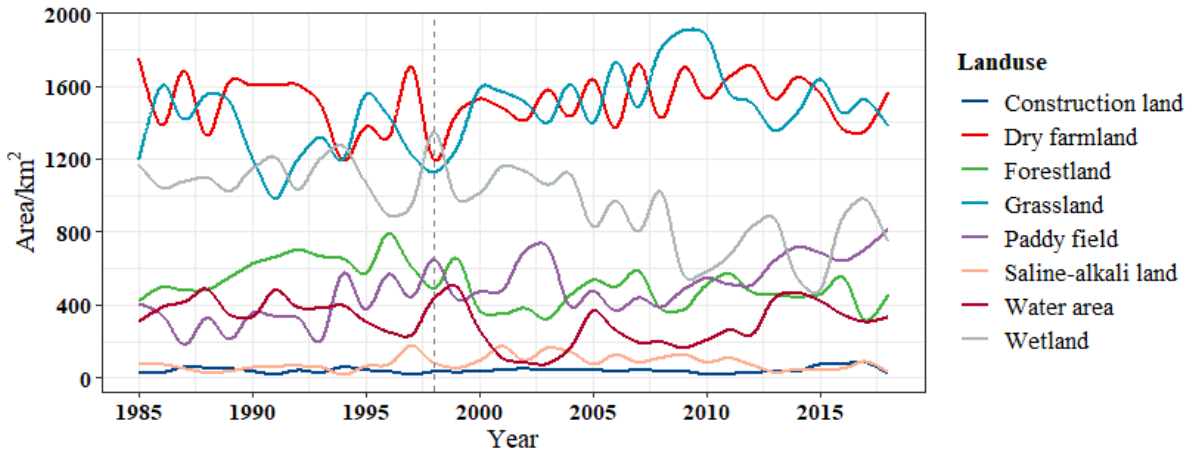

Figure S1. Characteristics of different land-use types from 1985 to 2018.

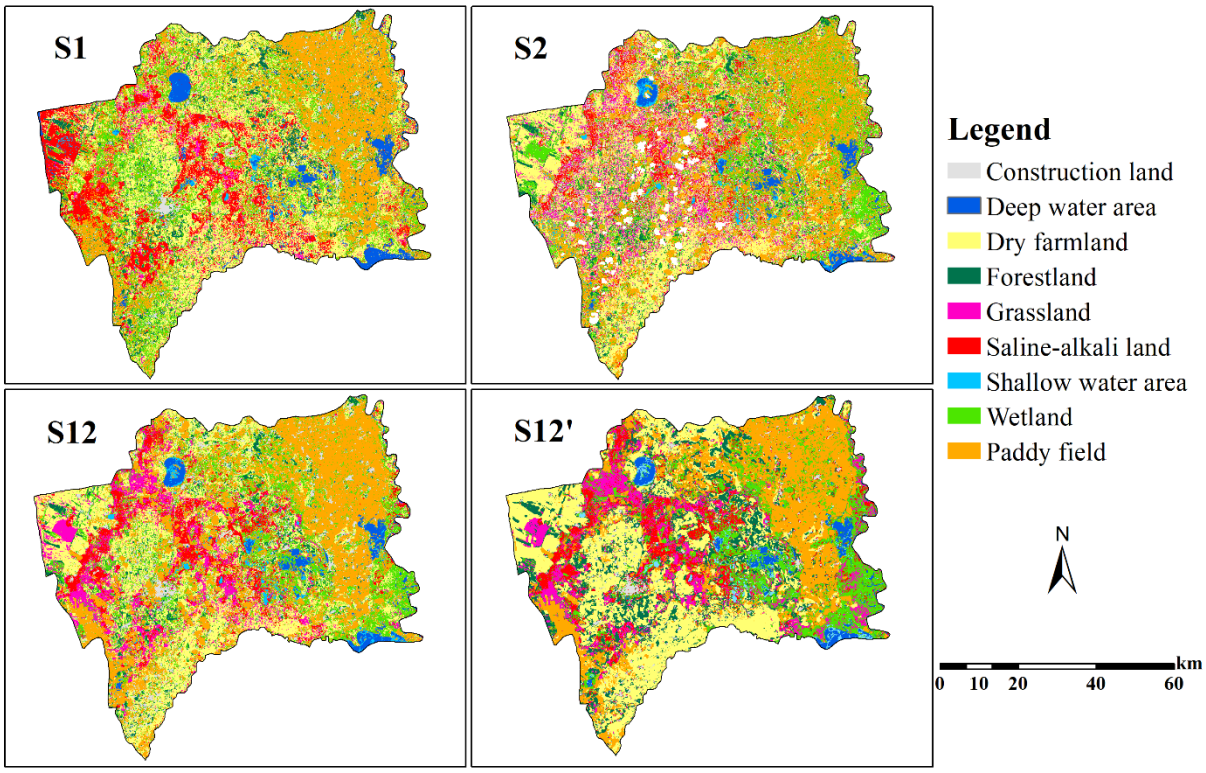

Figure S2. The land-use maps based on different data sources or methods. S1 is the land-use map based on Sentinel-1 data using dB, CC, and polarization decomposition method, S2 uses the vegetation and water indices of Sentinel-2 data, S12 is the combination of S1 and S2, S12' is based on S12 and multi-temporal analysis with Sentinel-1 data.

Reference

1. Mohammadimanesh, F., et al., *Multi-temporal, multi-frequency, and multi-polarization coherence and SAR backscatter analysis of wetlands.* ISPRS Journal of Photogrammetry and Remote Sensing, 2018. **142**: p. 78-93.
2. Pelich, R., et al., *EXPLORING DUAL-POLARIMETIC DESCRIPTORS FOR SENTINEL-1 BASED SHIP DETECTION*, in *Igarss 2018 - 2018 Ieee International Geoscience and Remote Sensing Symposium*. 2018. p. 2404-2407.
3. Liu, C.-A., et al., *Assessment of the X- and C-Band Polarimetric SAR Data for Plastic-Mulched Farmland Classification.* Remote Sensing, 2019. **11**(6).